

A CP-free STBC-MIMO OFDM communication system for underwater multipath channel

Shiho Oshiro
 Graduate School of Engineering and Science
 University of the Ryukyus
 Okinawa, Japan
 k188574@ie.u-ryukyu.ac.jp

Tomohisa Wada
 Dept. of Engineering, Area of Computer Science and Intelligent Systems
 University of the Ryukyus
 Okinawa, Japan
 wada@ie.u-ryukyu.ac.jp

Abstract— This paper proposes a Space Time Block Code (STBC) MIMO OFDM system without Cyclic Prefix (CP) but robust for long multipath echo channel, targeting the horizontal direction underwater communication. The system consists of two transmitting elements and more than 3 receiving elements. The configuration of STBC in this paper is 2×3 or 2×4 . STBC-OFDM symbol length is 32 ms with 512 sampling points. Under multipath condition without CP, Inter Symbol Interference (ISI) and Inter Carrier Interference (ICI) happens and causes severe communication performance degradation. In the proposed system, the ISI is removed by multiplying Left Null Space Vectors based on measured Channel Impulse Responses (CIRs) and the ICI is minimized by multiplying Minimum Mean Square Error (MMSE) weight. By increasing the number of receiving element (transducer), the Left Null Space Vectors can be obtained. To verify the ISI and ICI suppression performance, Matlab computer simulation is used. For 2×3 STBC-MIMO cases, roughly 150 (16QAM) and 190 (QAM) sampling points delayed multipath has been compensated successfully. For 2×4 STBC-MIMO cases, more than 250 (16QAM and QPSK) sampling points delayed multipath also compensated.

Keywords—Underwater Acoustic Communication, OFDM, STBC, MIMO

I. INTRODUCTION

Because of a progress in marine development for seabed natural resources such as hydrothermal deposits, methane hydrates, deep sea exploring becomes essential. Unlike onshore surveys, radio waves and sunlight do not reach the deep sea, and it is a high pressure environment. Therefore, we can not look into the sky using satellites. Techniques different from surveys by on-the-ground minerals and surveys by oil and gas resources surveys utilizing hygiene and boring are required. Especially, AUV (autonomous underwater vehicle) without any wires is demanded since its searching area is not

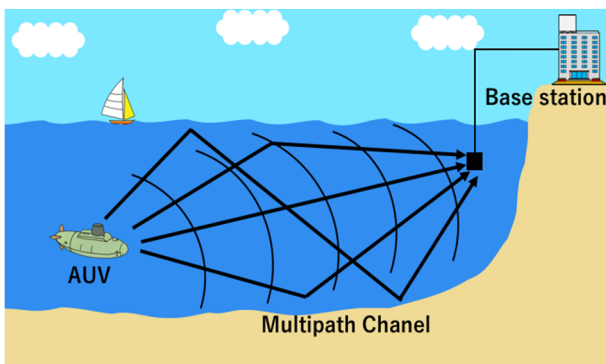


Fig. 1: Target application of STBC-MIMO communication system.

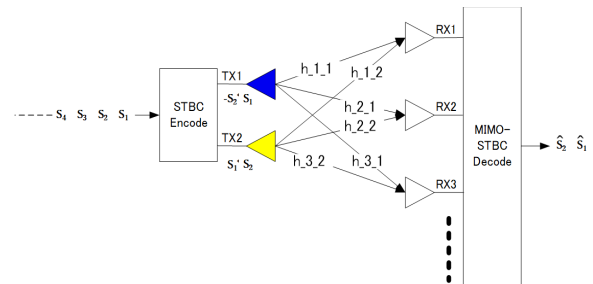


Fig. 2: Block Diagram of conventional STBC-MIMO communication system.

restricted by wire length. Then, wireless underwater communication has been become important to acquire AUV collected data without docking. Fig.1 shows a target application of the STBC-MIMO communication system. Since the signal propagation direction is horizontal, delayed signal is caused by reflection at the surface and bottom of the sea. By enabling high bandwidth wireless communication between AUV and base station, AUV can continue a deep seabed exploring without rendezvousing with the station.

In this paper, we propose an underwater acoustic STBC-MIMO OFDM communication system without cyclic prefix based on the algorithm in the papers [1-2]. Fig.2 shows the block diagram of STBC-MIMO OFDM system. The transmitter side has two elements while the receiver side equips more than 3 elements. At the transmitter side, Alamouti's code is used [3]. At the receiver side, STBC decode is performed with compensation of both Inter Symbol Interference (ISI) and Inter Carrier Interference (ICI) by heavy signal processing.

In the section II, at first conventional OFDM system with CP is shown. Then the proposed STBC-MIMO system architecture will be disclosed. The detail of the ISI and ICI compensation are also described. The section III shows simulated results for 3 and 4 elements receiver cases. Finally, the summary is concluded in section IV.

II. SYSTEM ARCHITECTURE

A. 1×1 conventional OFDM system with CP

Fig. 3 shows a block diagram of a conventional OFDM communication system. The upper side corresponds to transmitter and the lower side is receiver. First, bit information are modulated by PSK/QAM mapper. Then the mapped

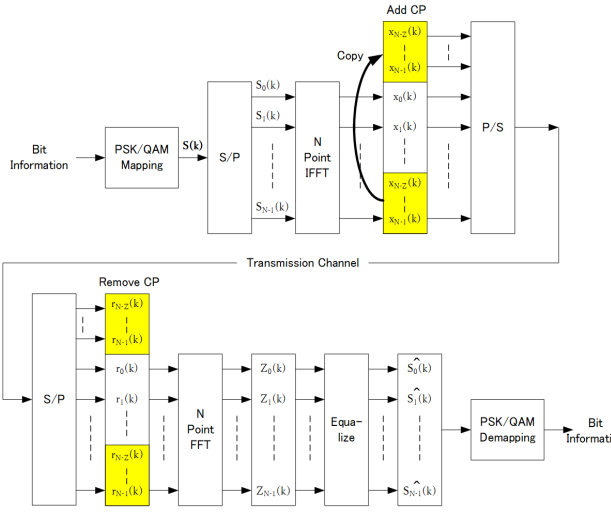


Fig. 3: Block Diagram of conventional 1x1 OFDM system with CP.

outputs are serial to parallel (S/P) converted to make N-symbols packet. The N-symbols frequency domain packet is IFFTed to make N-points time domain baseband OFDM symbol. As shown in yellow box, the tail parts are copied to the head as Cyclic Prefix (CP) addition. The purpose of CP is to remove ISI from the time delayed previous OFDM symbol to current OFDM symbol as far as the delay is smaller than CP length[1]. In the receiver side, reverse operation is performed. However, since multi-path transmission channel causes signal distortion, the Equalization process is applied for the FFT outputs in the receiver. To perform the equalization, transmission channel estimation (Channel Impulse Response or Channel Transfer Function estimation) is required but it is not included in Fig. 3.

B. CP free STBC-MIMO OFDM system

Fig. 4 shows CP free STBC-MIMO OFDM system. The $\mathbf{S}_1(k)$, $\mathbf{S}_2(k)$ are PSK/QAM modulated signal packets similar to the conventional OFDM. By STBC Alamouti's encoding, two time slots, two OFDM symbols are generated by two parallel IFFTs. At 1st time slot, $\mathbf{S}_1(k)$, $\mathbf{S}_2(k)$ are IFFTed to generate $\mathbf{x}_1(k)$, $\mathbf{x}_2(k)$ vectors. Then at 2nd time slot, $-\mathbf{S}_2^*(k)$, $\mathbf{S}_1^*(k)$ are IFFTed to generate $\mathbf{x}_1(k+1)$, $\mathbf{x}_2(k+1)$ vectors. $\mathbf{S}_1^*(k)$ is complex conjugate of $\mathbf{S}_1(k)$. Those two time slots are pairs for STBC encoding and decoding. Fig. 5 shows time-frequency representation of the STBC-MIMO OFDM signals. The used FFT/IFFT size is 512. Then each vertical line of circles corresponds to one OFDM symbol. To perform channel estimation Scattered Pilot (SP) symbols are inserted.

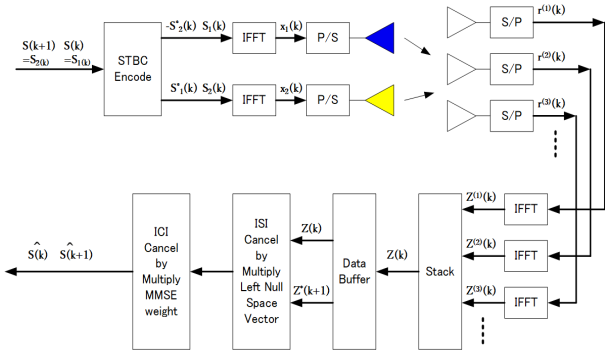


Fig. 4: Block diagram of CP free STBC-MIMO OFDM system.

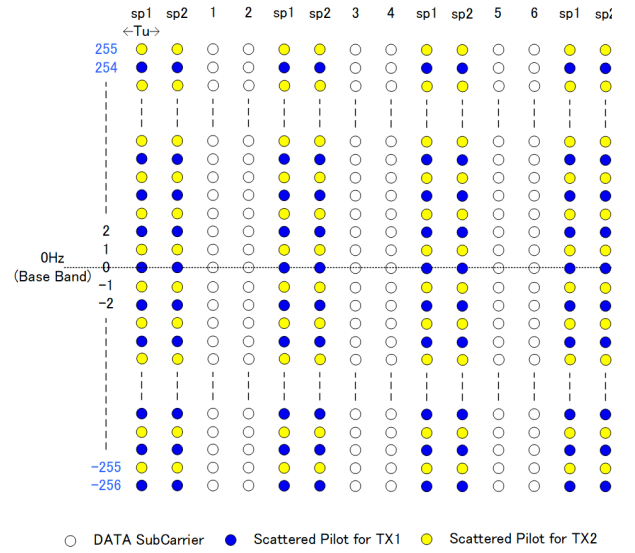


Fig. 5: Time-Frequency representation of STBC-MIMO OFDM. Every four symbols, Data of two OFDM symbols are placed and Scattered Pilots (SPs) of two OFDM symbols. The blue SPs are only for TX1

The blue subcarriers are only for blue transmit element (TX1) and the yellow subcarriers are for yellow transmit element (TX2) as shown in Fig. 4. The white circles corresponds to modulated symbol such as $\mathbf{S}_1(k)$, $\mathbf{S}_2(k)$.

The signal at m -th receiving element $\mathbf{r}^{(m)}(k)$ from two transmitting elements is shown in equation (1)[5]. \mathbf{F} is FFT matrix and \mathbf{F}^H is Hermitian matrix of \mathbf{F} . Then \mathbf{F}^H operation corresponds to IFFT. $h_l^{(m,i)}(k)$ is the channel impulse response between i -th transmitter to m -th receiver element. $\mathbf{H}_0^{(m,i)}(k)$ is upper triangular Toeplitz matrix, which corresponds to Delay in the same time= k OFDM symbol and $\mathbf{H}_1^{(m,i)}(k-1)$ is lower triangular Toeplitz matrix, which corresponds to Delay from the previous time= $k-1$ OFDM symbol. $\mathbf{n}^{(m)}(k)$ is additive white Gaussian noise.

$$\begin{aligned} \mathbf{r}^{(m)}(k) &= \begin{pmatrix} \mathbf{H}_1^{(m,1)}(k-1) & \mathbf{H}_0^{(m,1)}(k) \\ \mathbf{H}_1^{(m,2)}(k-1) & \mathbf{H}_0^{(m,2)}(k) \end{pmatrix} \begin{pmatrix} \mathbf{F}^H(-\mathbf{s}_2^*(k-1)) \\ \mathbf{F}^H \mathbf{s}_1(k) \end{pmatrix} \\ &+ \begin{pmatrix} \mathbf{H}_1^{(m,2)}(k-1) & \mathbf{H}_0^{(m,2)}(k) \\ \mathbf{H}_1^{(m,1)}(k-1) & \mathbf{H}_0^{(m,1)}(k) \end{pmatrix} \begin{pmatrix} \mathbf{F}^H \mathbf{s}_1^*(k-1) \\ \mathbf{F}^H \mathbf{s}_2(k) \end{pmatrix} + \mathbf{n}^{(m)}(k) \dots (1) \end{aligned}$$

$$\mathbf{H}_0^{(m,i)}(k) = \begin{pmatrix} h_0^{(m,i)}(k) & 0 & \dots & 0 & \dots & 0 \\ \vdots & \vdots & \ddots & \vdots & \ddots & \vdots \\ h_L^{(m,i)}(k) & \vdots & \vdots & 0 & \vdots & 0 \\ 0 & \vdots & \vdots & \vdots & h_0^{(m,i)}(k) & \vdots \\ \vdots & \vdots & \vdots & \vdots & \vdots & 0 \\ 0 & \dots & 0 & h_L^{(m,i)}(k) & \dots & h_0^{(m,i)}(k) \end{pmatrix} \dots (2)$$

$$\mathbf{H}_1^{(m,i)}(k-1) = \begin{pmatrix} 0 & \dots & 0 & h_L^{(m,i)}(k-1) & \dots & h_1^{(m,i)}(k-1) \\ \vdots & \vdots & \vdots & \vdots & \ddots & \vdots \\ 0 & \vdots & \vdots & 0 & \vdots & h_L^{(m,i)}(k-1) \\ \vdots & \vdots & \vdots & \vdots & \vdots & 0 \\ \vdots & \vdots & \vdots & \vdots & \vdots & \vdots \\ 0 & \dots & 0 & 0 & \dots & 0 \end{pmatrix} \dots (3)$$

By expanding equation (1), the following equation (4) is obtained.

$$\begin{aligned} \mathbf{r}^{(m)}(k) &= \sum_{i=1}^2 \left(\mathbf{H}_0^{(m,1)}(k) + \mathbf{H}_1^{(m,1)}(k) \right) \mathbf{F}^H \mathbf{s}_1(k) - \sum_{i=1}^2 \mathbf{H}_1^{(m,1)}(k) \mathbf{F}^H \mathbf{s}_1(k) \\ &+ \mathbf{H}_1^{(m,1)}(k-1) \mathbf{F}^H \mathbf{s}_1^*(k-1) - \mathbf{H}_1^{(m,2)}(k-1) \mathbf{F}^H \mathbf{s}_2^*(k-1) \\ &+ \mathbf{n}^{(m)}(k) \dots (4) \end{aligned}$$

After demodulation by FFT matrix F , the frequency domain received signal is given as equation (5). Since $\mathbf{H}_0^{(m,1)}(k) + \mathbf{H}_1^{(m,1)}(k)$ is circulant matrix, $\mathbf{D}^{(m,i)}(k)$ is diagonal matrix because of equation (6). From here, to simplify the equations, noise term is ignored.

$$\begin{aligned} \mathbf{z}^{(m)}(k) &= \mathbf{F}\mathbf{r}^{(m)}(k) = \sum_{i=1}^m \mathbf{F}(\mathbf{H}_0^{(m,1)}(k) + \mathbf{H}_1^{(m,1)}(k))\mathbf{F}^H\mathbf{s}_i(k) \\ &- \sum_{i=1}^2 \mathbf{F}\mathbf{H}_1^{(m,1)}(k)\mathbf{F}^H\mathbf{s}_i(k) + \mathbf{F}\mathbf{H}_1^{(m,1)}(k-1)\mathbf{F}^H\mathbf{s}_1^*(k-1) \\ &- \mathbf{F}\mathbf{H}_1^{(m,2)}(k-1)\mathbf{F}^H\mathbf{s}_2^*(k-1) + \mathbf{F}\mathbf{n}^{(m)}(k) \dots (5) \\ \mathbf{D}^{(m,i)}(k) &= \mathbf{F}(\mathbf{H}_0^{(m,1)}(k) + \mathbf{H}_1^{(m,1)}(k))\mathbf{F}^H \dots (6) \end{aligned}$$

By stacking $m=1$ to 3 in 3 elements receiver case, the following equation (7) is obtained.

$$\begin{aligned} \mathbf{z}(k) &= \begin{pmatrix} \mathbf{z}^{(1)}(k) \\ \mathbf{z}^{(2)}(k) \\ \mathbf{z}^{(3)}(k) \end{pmatrix} = \begin{pmatrix} \mathbf{D}^{(1,1)}(k) & \mathbf{D}^{(1,2)}(k) \\ \mathbf{D}^{(2,1)}(k) & \mathbf{D}^{(2,2)}(k) \\ \mathbf{D}^{(3,1)}(k) & \mathbf{D}^{(3,2)}(k) \end{pmatrix} \begin{pmatrix} \mathbf{s}_1(k) \\ \mathbf{s}_2(k) \end{pmatrix} - \mathbf{H}_{ICl}(k) \begin{pmatrix} \mathbf{s}_1(k) \\ \mathbf{s}_2(k) \end{pmatrix} \\ &+ \mathbf{H}_{ISl}(k-1) \begin{pmatrix} -\mathbf{s}_2^*(k-1) \\ \mathbf{s}_1^*(k-1) \end{pmatrix} \dots (7) \end{aligned}$$

Similarly, time= $k+1$ case can be obtained as follows. $\mathbf{0}$ is zero matrix.

$$\begin{aligned} \mathbf{z}(k+1) &= \begin{pmatrix} \mathbf{z}^{(1)}(k+1) \\ \mathbf{z}^{(2)}(k+1) \\ \mathbf{z}^{(3)}(k+1) \end{pmatrix} \\ &= \begin{pmatrix} \mathbf{D}^{(1,1)}(k+1) & \mathbf{D}^{(1,2)}(k+1) \\ \mathbf{D}^{(2,1)}(k+1) & \mathbf{D}^{(2,2)}(k+1) \\ \mathbf{D}^{(3,1)}(k+1) & \mathbf{D}^{(3,2)}(k+1) \end{pmatrix} \begin{pmatrix} -\mathbf{s}_2^*(k) \\ \mathbf{s}_1^*(k) \end{pmatrix} \\ &- \mathbf{H}_{ICl}(k+1) \begin{pmatrix} -\mathbf{s}_2^*(k) \\ \mathbf{s}_1^*(k) \end{pmatrix} + \mathbf{H}_{ISl}(k) \begin{pmatrix} \mathbf{s}_1(k) \\ \mathbf{s}_2(k) \end{pmatrix} \dots (8) \end{aligned}$$

$$\mathbf{H}_{ICl}(k) = \begin{pmatrix} \mathbf{F} & \mathbf{0} & \mathbf{0} \\ \mathbf{0} & \mathbf{F} & \mathbf{0} \\ \mathbf{0} & \mathbf{0} & \mathbf{F} \end{pmatrix} \begin{pmatrix} \mathbf{H}_1^{(1,1)}(k) & \mathbf{H}_1^{(1,2)}(k) \\ \mathbf{H}_1^{(2,1)}(k) & \mathbf{H}_1^{(2,2)}(k) \\ \mathbf{H}_1^{(3,1)}(k) & \mathbf{H}_1^{(3,2)}(k) \end{pmatrix} \begin{pmatrix} \mathbf{F}^H & \mathbf{0} \\ \mathbf{0} & \mathbf{F}^H \end{pmatrix} \dots (9)$$

$$\begin{aligned} \mathbf{H}_{ISl}(k-1) &= \begin{pmatrix} \mathbf{F} & \mathbf{0} & \mathbf{0} \\ \mathbf{0} & \mathbf{F} & \mathbf{0} \\ \mathbf{0} & \mathbf{0} & \mathbf{F} \end{pmatrix} \begin{pmatrix} \mathbf{H}_1^{(1,1)}(k-1) & \mathbf{H}_1^{(1,2)}(k-1) \\ \mathbf{H}_1^{(2,1)}(k-1) & \mathbf{H}_1^{(2,2)}(k-1) \\ \mathbf{H}_1^{(3,1)}(k-1) & \mathbf{H}_1^{(3,2)}(k-1) \end{pmatrix} \begin{pmatrix} \mathbf{F}^H & \mathbf{0} \\ \mathbf{0} & \mathbf{F}^H \end{pmatrix} \dots (10) \end{aligned}$$

$$\begin{aligned} \mathbf{H}_{ICl}(k+1) &= \begin{pmatrix} \mathbf{F} & \mathbf{0} & \mathbf{0} \\ \mathbf{0} & \mathbf{F} & \mathbf{0} \\ \mathbf{0} & \mathbf{0} & \mathbf{F} \end{pmatrix} \begin{pmatrix} \mathbf{H}_1^{(1,1)}(k+1) & \mathbf{H}_1^{(1,2)}(k+1) \\ \mathbf{H}_1^{(2,1)}(k+1) & \mathbf{H}_1^{(2,2)}(k+1) \\ \mathbf{H}_1^{(3,1)}(k+1) & \mathbf{H}_1^{(3,2)}(k+1) \end{pmatrix} \begin{pmatrix} \mathbf{F}^H & \mathbf{0} \\ \mathbf{0} & \mathbf{F}^H \end{pmatrix} \dots (11) \end{aligned}$$

$$\mathbf{H}_{ISl}(k) = \begin{pmatrix} \mathbf{F} & \mathbf{0} & \mathbf{0} \\ \mathbf{0} & \mathbf{F} & \mathbf{0} \\ \mathbf{0} & \mathbf{0} & \mathbf{F} \end{pmatrix} \begin{pmatrix} \mathbf{H}_1^{(1,1)}(k) & \mathbf{H}_1^{(1,2)}(k) \\ \mathbf{H}_1^{(2,1)}(k) & \mathbf{H}_1^{(2,2)}(k) \\ \mathbf{H}_1^{(3,1)}(k) & \mathbf{H}_1^{(3,2)}(k) \end{pmatrix} \begin{pmatrix} \mathbf{F}^H & \mathbf{0} \\ \mathbf{0} & \mathbf{F}^H \end{pmatrix} \dots (12)$$

Using the \mathbf{J} matrix, equations (7) and (8) can be expressed as equation (14). \mathbf{I} matrix is unit matrix.

$$\mathbf{J} = \begin{pmatrix} \mathbf{0} & -\mathbf{I} \\ \mathbf{I} & \mathbf{0} \end{pmatrix} \dots (13)$$

The equation (14) corresponds to the outputs of data buffer in Fig. 4. After data buffer, ISI and ICI components, which is the last term of equation (14) will be removed by two stages additional signal processing[7].

$$\begin{aligned} \tilde{\mathbf{z}}(k+1) &= \begin{pmatrix} \mathbf{z}(k) \\ \mathbf{z}^*(k+1) \end{pmatrix} \\ &= \begin{pmatrix} \mathbf{D}^{(1,1)}(k) & \mathbf{D}^{(1,2)}(k) \\ \mathbf{D}^{(2,1)}(k) & \mathbf{D}^{(2,2)}(k) \\ \mathbf{D}^{(3,1)}(k) & \mathbf{D}^{(3,2)}(k) \end{pmatrix} \begin{pmatrix} \mathbf{s}_1(k) \\ \mathbf{s}_2(k) \end{pmatrix} \\ &+ \begin{pmatrix} [-\mathbf{H}_{ICl}(k) & \mathbf{H}_{ISl}(k-1) \cdot \mathbf{J}] \begin{pmatrix} \mathbf{s}_1(k) \\ \mathbf{s}_2(k) \\ \mathbf{s}_1^*(k-1) \\ \mathbf{s}_2^*(k-1) \end{pmatrix} \\ \dots \\ [-\mathbf{H}_{ICl}^*(k+1) \cdot \mathbf{J} & \mathbf{H}_{ISl}^*(k)] \begin{pmatrix} \mathbf{s}_1(k) \\ \mathbf{s}_2(k) \\ \mathbf{s}_1^*(k) \\ \mathbf{s}_2^*(k) \end{pmatrix} \end{pmatrix} \dots (14) \\ \mathbf{D}(k) &= \begin{pmatrix} \mathbf{D}^{(1,1)}(k) & \mathbf{D}^{(1,2)}(k) \\ \mathbf{D}^{(2,1)}(k) & \mathbf{D}^{(2,2)}(k) \\ \mathbf{D}^{(3,1)}(k) & \mathbf{D}^{(3,2)}(k) \end{pmatrix} \dots (15) \end{aligned}$$

Summary of the STBC-MIMO OFDM system feature is shown in Table I. OFDM symbol length T is 32.0 ms, which corresponds to 512 sampling points and subcarrier spacing is 31.25Hz.

TABLE I: COMMUNICATION SYSTEM FEATURE

Parameters	Value
Receiver	3 or 4 Transducers
Transmitter	2 Transducers
Sampling Frequency	16.0 kHz
Band Width	± 8 kHz (16KHz)
FFT size	512
OFDM symbol length T	32.0 ms
Guard Interval (Cyclic prefix)	none
Sub-carrier spacing	31.25 Hz
Number of sub-carrier	512
Pilot OFDM symbol	50%
Data OFDM symbol	50%
Carrier Modulation	QPSK/16QAM
Max. Dara Rate w/o FEC	32 kbps (16QAM) 16 kbps (QPSK)

C. ISI and ICI compensation

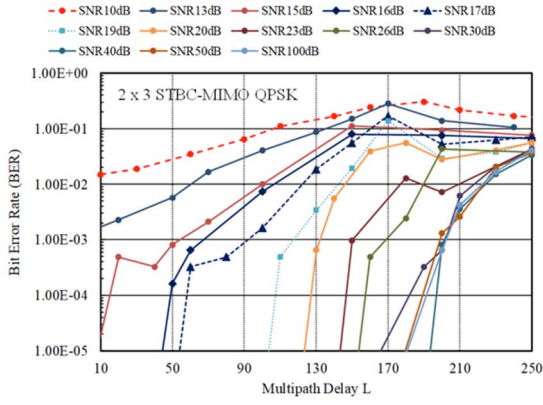
At first, to cancel the ISI component, the following $\mathbf{T}(k+1)$ matrix is generated as shown in equations (16-18). The columns of $\mathbf{T}_1(k+1)$ and $\mathbf{T}_2(k+1)$ are an orthogonal basis of Left Null Space of $[-\mathbf{H}_{ICl}(k) \quad \mathbf{H}_{ISl}(k-1)]$ and $[-\mathbf{H}_{ICl}^*(k+1)\mathbf{J} \quad \mathbf{H}_{ISl}^*(k)]$, respectively.

$$\mathbf{T}(k+1) = \begin{bmatrix} \mathbf{T}_1(k+1) \\ \mathbf{T}_2(k+1) \end{bmatrix} \dots (16)$$

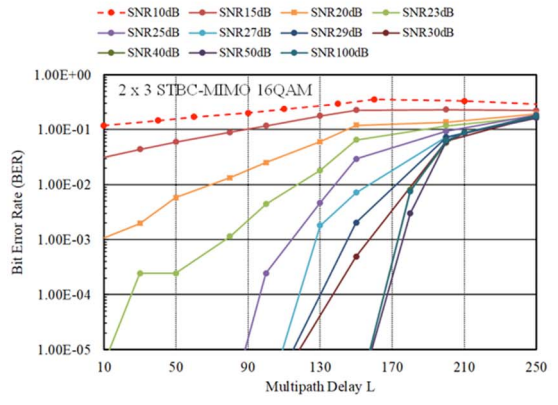
$$\mathbf{T}_1^H(k+1)[- \mathbf{H}_{ICl}(k) \quad \mathbf{H}_{ISl}(k-1)] = \mathbf{0}, \mathbf{T}_1^H(k+1)\mathbf{T}_1(k+1) = \mathbf{I} \dots (17)$$

$$\mathbf{T}_2^H(k+1)[- \mathbf{H}_{ICl}^*(k+1)\mathbf{J} \quad \mathbf{H}_{ISl}^*(k)] = \mathbf{0}, \mathbf{T}_2^H(k+1)\mathbf{T}_2(k+1) = \mathbf{I} \dots (18)$$

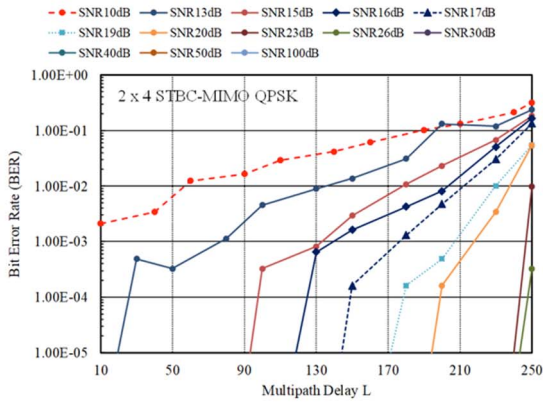
By multiplying $\mathbf{T}(k+1)$ to equation (14) from left, ISI component can be erased as equation (19).



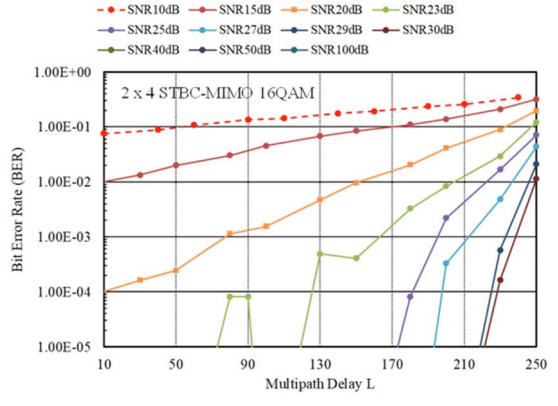
(a) QPSK, 3 element receivers



(a) 16QAM, 3 element receivers



(b) QPSK, 4 element receivers



(b) 16QAM, 4 element receivers

Fig. 6: QPSK simulated results

Fig. 7: 16QAM simulated results

$$\begin{aligned} \mathbf{T}(k+1)\tilde{\mathbf{z}}(k+1) &= \mathbf{T}(k+1) \begin{pmatrix} \mathbf{z}(k) \\ \mathbf{z}^*(k+1) \end{pmatrix} \\ &= \mathbf{T}(k+1) \begin{pmatrix} \mathbf{D}(k) \\ \mathbf{D}^*(k+1) \cdot \mathbf{J} \end{pmatrix} \begin{pmatrix} \mathbf{s}_1(k) \\ \mathbf{s}_2(k) \end{pmatrix} \dots \quad (19) \end{aligned}$$

After this, by multiplying $\mathbf{W}_{MMSE}(k+1)$ weight to equation (19), STBC decoded estimated $\hat{\mathbf{s}}_1(k)$ and $\hat{\mathbf{s}}_2(k)$ can be obtained as shown in equations (20-21).

$$\begin{pmatrix} \hat{\mathbf{s}}_1(k) \\ \hat{\mathbf{s}}_2(k) \end{pmatrix} = \mathbf{W}_{MMSE}(k+1)\mathbf{T}(k+1)\tilde{\mathbf{z}}(k+1) \dots \quad (20)$$

$$\begin{aligned} \mathbf{W}_{MMSE}(k+1) &= \left(\mathbf{T}^H(k+1) \begin{pmatrix} \mathbf{D}(k) \\ \mathbf{D}^*(k+1) \cdot \mathbf{J} \end{pmatrix} \begin{pmatrix} \mathbf{D}(k) \\ \mathbf{D}^*(k+1) \cdot \mathbf{J} \end{pmatrix}^H \mathbf{T}(k+1) \right. \\ &\quad \left. + 2\sigma^2 \mathbf{I} \right)^{-1} \mathbf{T}^H(k+1) \begin{pmatrix} \mathbf{D}(k) \\ \mathbf{D}^*(k+1) \cdot \mathbf{J} \end{pmatrix} \dots \quad (21) \end{aligned}$$

The 3 element receiver case has been shown so far. However, similarly, 4 element receiver also can be realized. In the following section, 3 and 4 element receiver cases are examined by computer simulation program Matlab.

III. COMPUTER SIMULATION

In order to verify ISI and ICI suppression performance of the proposed system, 2 x 3 and 2 x 4 STBC-MIMO configurations are simulated. As explained in the previous section, estimation of $\mathbf{H}_0^{(m,i)}(k)$ and $\mathbf{H}_1^{(m,i)}(k-1)$ matrixes are essential. In the simulation, SP OFDM symbols as shown in blue and yellow in Fig. 5 are used for channel estimation. In the simulation, two path multipath channel (one reflection)

is assumed and multipath delay L is used as key parameter. Detail of simulation condition is written in Table II.

TABLE II : Computer Simulation Conditions

Parameters	Value
STBC-MIMO configuration	2 x 3 or 2 x 4
Channel Model	2 path multipath
Desired / Undesired Ratio (DUR)	5~10dB
Multipath Delay L	< 256 point (16ms) 1point=62.5us
SNR(dB)	10 - 100 dB
Data Modulation	QPSK/16QAM

Fig. 6 shows the simulation result for QPSK for (a) 2 x 3 STBC-MIMO and (b) 2 x 4 STBC-MIMO cases. The vertical axis is Bit Error Rate (BER) and the horizontal axis is Multipath Delay Length in sampling period. Because of sampling frequency = 16kHz, 256 point delay L corresponds to 16 ms delay. For (a) 2 x 3 STBC-MIMO case, maximum delay L with BER < 1E-4 is roughly 190 sampling points even very high SNR such as 100dB. However, by increasing the number of element at receiver from 3 to 4 as shown in (b), maximum delay L is improved. In condition of SNR=26dB, roughly 240 sampling point multipath can be suppressed by the

proposed CP free STBC-MIMO system. Fig. 7 shows the 16QAM case. For (a) 2 x 3 STBC-MIMO case, maximum delay looks like limited less than 170 sampling points. However, by increasing the number of element at receiver from 3 to 4, even 30dB SNR case shows 220 sampling point delay has achieved.

In Fig. 8, simulated results are summarized. By increasing the number of element at receiver, allowable maximum delay L is improved. In conventional OFDM, multipath delay which exceeding the CP length causes severe BER degradation. However, in the proposed system, even CP free OFDM has indicated no severe performance degradation.

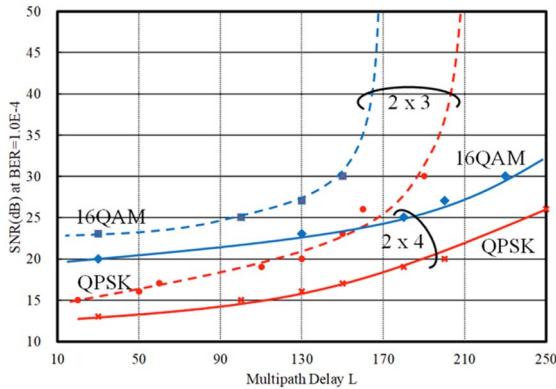


Fig. 8: Block diagram of CP free STBC-MIMO OFDM system.

IV. CONCLUSION

A STBC-MIMO OFDM system without CP but robust for long multipath echo channel is proposed. The system is targeting the horizontal direction underwater communication between AUV and mother ship / base stations because of many reflection at the surface and bottom of the sea. The configuration of STBC in this paper is 2 x 3 or 2 x 4 and the symbol length is 32 ms with 512 baseband sampling points.

Under multipath condition without CP, Inter Symbol Interference (ISI) and Inter Carrier Interference (ICI) happens and causes severe communication performance degradation. In this system, the ISI is removed by multiplying Left Null Space Vector based on measured Channel Impulse Responses (CIRs) and the ICI is minimized by multiplying Minimum Mean Square Error (MMSE) weight[4]. By increasing the number of receiving element (transducer), the Left Null Space Vector can be obtained.

To verify the ISI and ICI suppression performance, Matlab computer simulation is used. For 2 x 3 STBC-MIMO cases, roughly 150 (16QAM) and 190 (QAM) sampling points delayed multipath has been compensated successfully. For 2 x 4 STBC-MIMO cases, more than 250 (16QAM and QPSK) sampling points delayed multipath also successfully compensated.

REFERENCES

- [1] Chih-Yuan LIN, Jwo-Yuh WU, Ta-Sung LEE, "A Near-Optimal Low-Complexity Transceiver for CP-Free Multi-Antenna OFDM Systems," *IEICE TRANS.COMMUN.*, VOL E89-B, NO.1, JANUARY 2006.
- [2] Chih-Wei Wu, Shiunn-Jang Chern, "Novel Frequency Domain DFE with Oblique Projection for CP Free ST-BC MIMO OFDM System," Master Thesis at National Sun Yat-sen University, June 2009.
- [3] S.M. Alamouti, "A simple transmit diversity technique for wireless communications". *IEEE Journal on Selected Areas in Communications*. 16 (8): 1451–1458, October 1998.
- [4] A. Stamoulis, G. B. Giannakis, A. Scaglione, "Block FIR Decision-Feedback Equalizers for Filterbank Precoded Transmissions with Blind Channel Estimation Capabilities," *IEEE Trans. Comm.*, Vol. 49, no. 1, pp.69-83, Jan. 2001.
- [5] X.D. Wang and G.B. Giannakis, "Wireless multicarrier communications," *IEEE Signal Process. Mag.*, vol.17, no.3, pp.29–48, May 2000.
- [6] Li Zhang, Mathini, Sellathurai, Jonathon and Chambers, "An Iterative Multiuser Receiver for Space-Time Coded MIMO-OFDM System", Centre of Digital Signal Processing, Cardiff University, Queen's Buildings, Cardiff CF24 3AA, Wales UK
- [7] Bertrand Muquet, Zhengdao Wang, Georgios B. Giannakis, Marc de Courville, and Pierre Duhamel, "Cyclic Prefixing or Zero Padding for Wireless Multicarrier Transmissions?" *IEEE TRANSACTIONS ON COMMUNICATIONS*, VOL. 50, NO. 12, DECEMBER 2002.